Efficient, Scalable Clarification of Diverse Bioprocess Streams

Using a Novel Pilot-Scale Tubular Bowl Centrifuge

Russ Lander, Chris Daniels, and Francis Meacle

Centrifugation is ubiquitous in the biotechnology industry, primarily in cell harvest and cell lysate clarification. The technology provides advantages over microfiltration, particularly for large macromolecules such as vaccines that are either virus-like particles or loosely structured polysaccharides or nucleic acids. When large pore-size cutoffs are needed, membranes are susceptible to filter fouling by cell debris. Scale-up can become problematic due to uncertain modeling of the fouled condition, as witnessed by the development of complex operational algorithms such as Cwall (**1**) and optimized flow patterns such as backpulsing (**2**) and co-current flow (**3**). Clarification by centrifugation, on the other hand, circumvents the problem altogether and eliminates the cost of batch filter replacement.

Several centrifuge designs are used to clarify biological streams, with scroll decanters, disc-stack centrifuges, and tubular bowl centrifuges being the most common. The choice for a given application depends on the nature and concentration of solid particles to be sedimented. For example, because of low sedimentation forces, the use of scroll decanters is limited to streams containing large particles such as mycelia or flocculated cells (**4**).

Disc-stack centrifuges can generate much higher centrifugal forces, process large volumes of material, and handle large quantities of solids, discharging sediment as a wet slurry (**5**). That can be either ejected continuously (nozzle discharge) or intermittently (solids ejecting discharge). Disc-stack centrifuges fit a wide range of uses in bioprocessing and have long been used to harvest microbial cells and inclusion bodies (**4**) or to clarify cell lysates (**12**).

A relatively new application for disc-stack centrifuges is in mammalian cell harvest, for which low expression rates of therapeutic proteins in cell culture (<2 g/L) require large volumes of cell cultures to be produced at manufacturing scale (>15,000-L bioreactors). The high throughput of disc-stack machines makes them a good choice at manufacturing scale (**5–11**). But mammalian cells are shear sensitive (**8**), so the high-shear entrance region of such machines was redesigned with a hydrohermetic seal to eliminate a problematic gas–liquid interface. Even so, careful operation is critical to preventing high fluid stress. Centrifuges must generally be operated at less than full speed to achieve optimum centrate clarity in mammalian cell harvest (**10, 11**).

Photo 1: Celeros tubular-bowl centrifuge (www.celeros-separations.com)

Biotech companies must quickly convert new leads into purified therapeutics for clinical trials and, ultimately, for the market. A key element in that process is the dual role of pilot facilities: to make GMP-compliant material for clinical trials and demonstrate process scale-up

Product Focus: All biologics

Process Focus: Downstream processing

Who Should Read: Process development, product development, manufacturing, QA/QC

Keywords: Centrifugation, shear, scale-up, clarification,

Level: Intermediate

Figure 2: Clarification as a function of feed rate and calculated value of Sigma (Equation 5) using conditions from Table 1

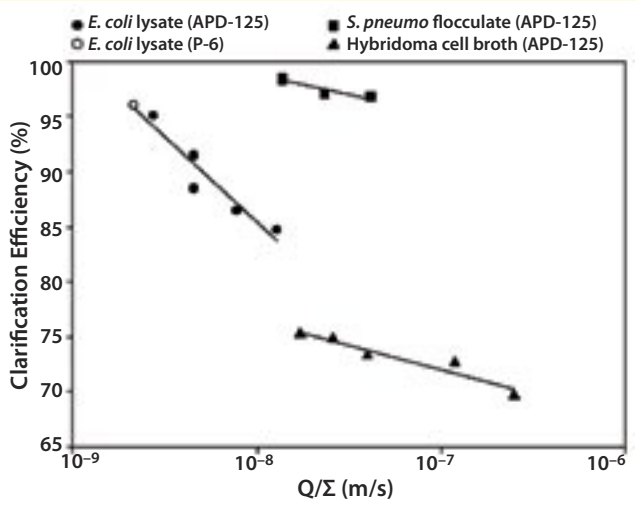

Figure 3: CHO clarification; relative concentration of DNA and absolute cell count in the centrate as a function of centrifuge speed during mammalian cell harvest; DNA concentration is shown relative to DNA concentration in the starting cell broth

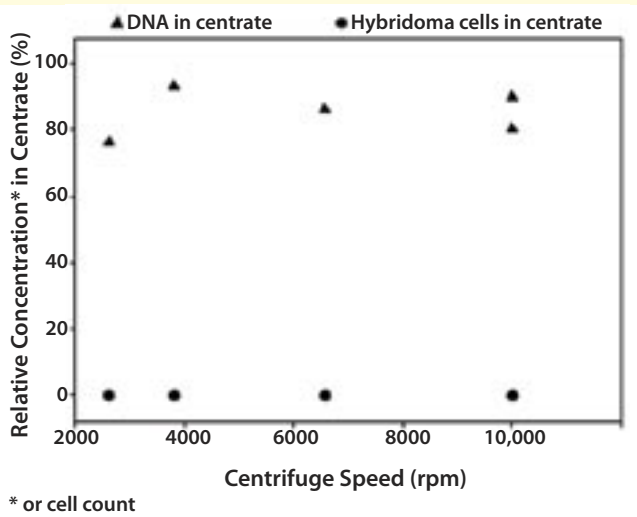

Figure 4: CHO cell clarification; CASY particle size analysis for centrifuge feed, paste, and centrate. Feed consisted of 10-µm cells and debris, paste consisted of intact cells, and centrate consisted of only cell debris

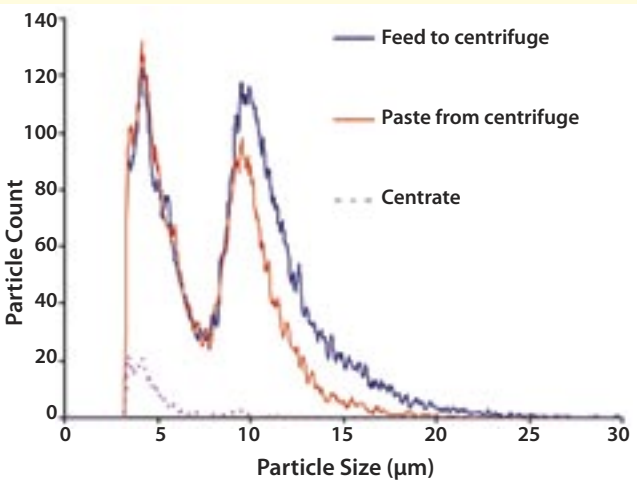

essential to manufacturing plant design. With an ever-increasing range of biologics (therapeutic proteins and fragments, peptides, viruses and viral capsids, naked DNA, and polysaccharides) expressed by a number of host cells (bacterial, yeast, mammalian, insect, and plant cells), the industry needs a versatile, scalable solid–liquid separator to process drugs for clinical studies.

Centrifugation meets those requirements and will no doubt gain in popularity. However, choosing a centrifuge for a multiproduct pilot-scale facility is not straightforward. Because they eject solids as a slurry, disc-stack machines cannot produce a dry centrifuge "cake." That imposes limitations on the recovery of liquid product from high–cell-density lysates and precludes the downstream separation of highly purified, precipitated product solutions. Tubular bowl centrifuges, effective in those regards, cannot process large volumes of cell lysate because of the large internal occupancy of their discharge scrapers and their lower separation surface area than disc-stack machines.

Selecting a centrifuge should include consideration of some very important additional criteria specific to bioprocessing: steam–in-place (SIP) and clean-in-place (CIP) capability to very stringent specifications and, or for many applications, the ability to contain aerosols (biocontainment) (**13**). Simplicity of equipment design is a common objective that emerges from such considerations.

We report here on pilot-scale testing of a new tubular bowl machine, the Model APD centrifuge from Celeros, Inc. (www.celeros-separations.com) shown in Photo 1. This model is designed for semicontinuous discharge of a dry solids cake, and its design allows CIP, SIP, and biocontainment. The machine has a low-shear feed design with a novel, straight-through, highly efficient, piston-type solids discharge mechanism. This design permits a narrow bowl construction, free of internal baffles, which resembles the traditional Sharples style geometry. Additionally, the upward flow pattern, low-shear feed cone, and underflow drawoff combine to promote a more flooded, lower shear feed condition and a stable, high-area liquid pool for optimal separations.

We assessed the clarification capabilities of the APD-125 centrifuge with a variety of biological process streams: whole cell and yeast lysates, Gram-positive and -negative microbial lysates, and Chinese hamster ovary (CHO) mammalian cells. We challenged the vendor's low-shear claim with mammalian cell lysates and certain shear-sensitive macromolecules: polysaccharides and plasmid DNA.

Materials and Methods

The test centrifuge was provided by RB Carr Engineering (now Celeros, Inc., of Novi, MI). This model is a fully automated, solid-bowl centrifuge capable of periodically discharging solids by a piston discharge mechanism. The bowl volume is 5.0 L, and its maximum rotational speed is 17,000 rpm (20,000 *g*). Our Pilot P6 model is a 1-L Powerfuge from Carr Separations (Franklin, MA), which lacks the bowl discharge capability. It was operated at 13,300–15,300 rpm (15,000–20,000 *g*).

The Sigma Model

Throughput and Clarification Analysis: Clarification is a function of the applied *g*-force and flow rate as well as bowl size and geometry. Centrifuge data are conveniently expressed by the Sigma correlation, which captures all operating and equipment variables. The separation capability of a centrifuge is characterized by a Sigma factor (Σ), which represents the area of a gravity settler required to achieve the same separation. The general form is expressed in Equation 1, where ω is the bowl speed, L is the bowl height, R is a characteristic radius of the pool and/or bowl, and G_c is acceleration due to gravity.

$$\Sigma = \frac{(L \times R) \times (\omega^2 R)}{G_c} \times \text{Geometric Factors}$$

$$\Sigma = (\text{area}) \times (\text{settling relative to gravity})$$

$$\Sigma = \frac{\pi\omega^2 L}{G} \times \frac{R_2^2 - R_1^2}{Ln\,(2R_2^2 \div (R_2^2 + R_1^2))}$$

In particular, for tubular bowl centrifuges, Σ is given by Equation 2, where R_1 and R_2 are radii of the pool and bowl, respectively (4).

To achieve a given separation in a continuous gravity settler, a settler must accommodate the characteristic particle settling velocity ($V_{particle}$) through a combination of flow rate (Q) and settler cross sectional area (A), as in Equation 3.

$$V_{eq.grav.} = \frac{Q}{\text{area}}$$

Using that analogy with the centrifugal separator (substituting the Σ expression for the equivalent area) provides a velocity expression corresponding to the removal of particles that settle at the given velocity or greater in a normal gravitational field (Equation 4).

$$V_{eq.centrif.} = \frac{Q}{\Sigma}$$

Substituting Equation 1 into Equation 4 yields Equation 5. The ratio Q/Σ represents a cutoff value of settling velocity for particles that can be separated in a centrifuge at specified conditions (Σ and flow rate). Particles with a Stokes gravity settling velocity greater than Q/Σ will be captured.

If the model is correct, clarification data for any flow rate and *g*-force should collapse to a single curve when plotted against V_{eq}. Even data for various types of centrifuges can be included if the correct Σ expressions are used (18). Such a plot can be used to predict maximum throughput for any clarification in a given centrifuge as well as scale-up to larger size equipment. Based on Ambler's derivation (19), the linear form for this plot is actually *Ln* (clarification) rather than *Ln* (Q/Σ) because settling times vary by several logs throughout a settling zone.

$$V_{eq.centrif.} = \frac{Q}{\left(\frac{\pi\omega^2 L}{G} R_2^2 - R_1^2\right) \div (Ln\,(2R_2^2 \div R_2^2 + R_1^2))}$$

Fermentation lysates of *Escherichia coli* and *Streptococcus pneumoniae* came from Merck and Co., Inc. (www.merck.com), which also provided harvested CHO cells. Purified pneumococcal capsular polysaccharide (serotype 23F, MW = 1.64×10^6 Da derived from *S. pneumoniae*) is a component of Merck's Pneumovax 23 vaccine. Plasmid DNA (8.6 kbp) was also obtained from Merck.

Clarification of Bacterial and Mammalian Cell Lysates: To determine throughput, we clarified a lysate of *E. coli*, a flocculated *S. pneumoniae* lysate, and a mammalian cell broth at differing feed rates and centrifuge bowl speeds. Steady state was established at each flow rate by feeding several bowl volumes, with periodic sampling to measure the turbidity of the clarified liquid. To test the validity of our performance correlation, we also clarified flocculated *E. coli* lysate using the 1-L Powerfuge machine.

Shear Challenge: Plasmid DNA and polysaccharide are both sensitive to shear (14, 15). We processed solutions of both at 15,000 *g* (14,722 rpm), duplicating the *g*-force that caused polysaccharide breakage in a P24 Powerfuge-type centrifuge (16). The 1 g/L Type 23F polysaccharide was subjected to a single pass at 1.0 Lpm (liters per minute, two minutes bowl residence time). *E. coli* lysate containing soluble plasmid DNA was subjected to five passes in the APD-125 at 15,000 *g* and a feed rate of 1 Lpm (4 min residence time).

To harvest intact mammalian cells, we used a full bowl startup condition to prevent any abrupt shear in the unwetted feed zone. To keep from shearing soluble polysaccharides, we fitted the discharge mechanism with a low-shear weir, which was not used in the case of the plasmid DNA test. (This weir is a cylinder with four rectangular openings of 10-mm width fitted at the top of the rotating bowl.)

Analytical Techniques: Turbidity was measured with a DRT-15CE turbidimeter from HF Scientific, Inc. (www.hfscientific.com). For estimating the yield loss of soluble product in the solid waste stream, after bowl paste was discharged with a scraper blade we weighed and analyzed it for liquid content. In the shear-sensitivity challenge using mammalian CHO cells, the viable (10 µm) cell population size distribution of collected solids was measured with a CASY TTC cell counter from Scharfe System GmbH (Reutlingen, Germany).

We measured cell breakage indirectly by detecting the release of DNA with a fluorescence-based Picogreen dye assay (Invitrogen Molecular Probes, http://probes.invitrogen.com). Disposition of 10-µm mammalian cells was visualized by differential interference contrast microscopy using an AX70 microscope from Olympus America Inc. (www.olympusamerica.com). We measured polysaccharide size reduction by high-performance size-exclusion chromatography with laser light scattering detection according to the method of Bednar (17). Using a Dawn laser photometer and interferometric refractometer from Wyatt Technology (www.wyatt.com), plasmid DNA breakage was measured by sodium-dodecyl sulfate polyacrylamide gel electrophoresis (SDS-PAGE) and a scanning densitometer from New England Biolabs Inc. (www.neb.com), which showed plasmids broken into relaxed, open circles as well as broken host-cell genomic DNA. For modeling and scale-up projection mathematics of throughput and shear, see the "Sigma Model" box.

Figure 5: Shear challenge (plasmid DNA); agarose gel showing the amount of plasmid and chromosomal DNA as a function of the number of passes through the centrifuge at 15,000 *g*

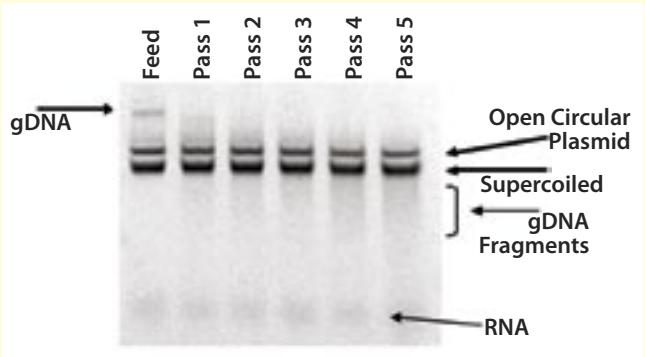

Figure 6: Shear challenge (polysaccharides); PnP size before and after being passed through the centrifuge.; no change in size or polydispersity

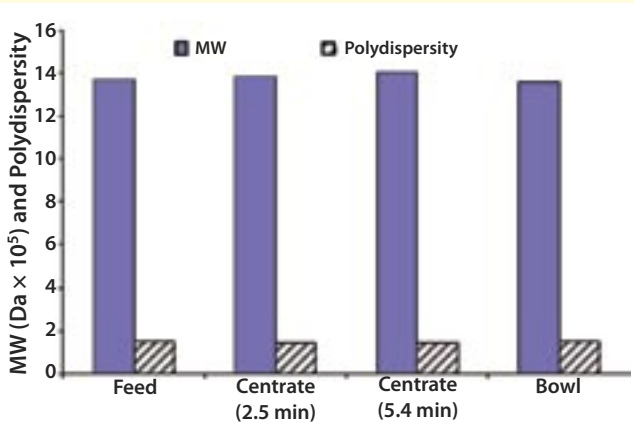

Results

Throughput and Clarification

Efficiency: Table 1 summarizes experiments examining the effects of centrifuge speed and feed rate on clarification efficiency. The same results are plotted in Figure 2 as clarification efficiency against *Ln* (Q/Σ). Derivation and application of Σ to scale-up of our APD-125 data is described in the "Sigma Model" box. Figure 2 shows that particles of flocculated *S. pneumoniae* lysate were easiest to clarify, with over 98% clarification efficiency at a Q/Σ of 10^{-8} m/s. High flocculation efficiency is achieved
at all values of Q/Σ, implying that the flocculation was successful in making a uniformly large population of solids that were degraded to inseparable fines by shear in the centrifuge.

For the more highly viscous and nonflocculated *E. coli* lysate, a much lower value of Q/Σ (10^{-9} m/s) was required to reach 95% clarification efficiency and the clarification was quite sensitive to Q/Σ. Efficiency for the mammalian cell broth was only 70–75% over the range of Q/Σ values examined. However such low values misrepresent the quality of separation for intact cells. CASY particle size analysis showed that all mammalian cells were removed from the centrate at all conditions tested. Moreover, as shown below, cells were not degraded. So variation in clarification at the indicated range of Q/Σ represents removal of cell debris that were originally present in the feed.

As Figure 2 shows, Sigma analysis accurately incorporates additional data obtained using a smaller centrifuge (batch type model). The P6 Powerfuge is about 20% of the APD-125's bowl volume. Such straightforward scale-up suggests that the semicontinuous APD attains good bowl pool integrity.

Table 1: Clarification of bioprocess streams as a function of feed rate and speed using APD-125 model

Material	G-Force (*g*)	Feed Rate (Lpm)	Q/Σ (m/s)	Clarification(%)
E. coli lysate	15,000	0.6	2.8^{-9}	95.0
	15,000	1.0	4.6^{-9}	91.4
	15,000	1.0	4.6^{-9}	88.4
	15,000	1.7	7.8^{-9}	86.4
	15,000	2.8	1.3^{-8}	84.7
S. pneumoniae flocculate	5,000	1.0	1.4^{-8}	98.5
	5,000	1.0	1.4^{-8}	98.3
	5,000	1.7	2.3^{-8}	97.0
	5,000	3.0	4.1^{-8}	96.8
Hybridoma cell broth	8,000	2.0	1.7^{-8}	75.3
	8,000	3.0	2.6^{-8}	74.8
	3,448	2.0	4.0^{-8}	73.3
	1,155	2.0	1.2^{-7}	72.7
	550	2.0	2.5^{-7}	69.7

Process Yield Limited By Solids Desiccation: Because the goal of most centrifugation steps is a solid–liquid separation, any residual liquid in the centrifuge cake adversely affects efficiency by reducing either yield (soluble products) or purification efficiency (insoluble products). A strategic conflict arises between the objectives of high cell density in fermentation and yield because of entrained liquid in a high–cell-mass waste stream.

In our APD tests, *E. coli* and *S. pneumoniae* cells were discharged as integral pastes containing only 73.6% and 69.8% entrained liquid respectively (350–430 grams of dry solids per liter of cake liquid), which corresponds to product yields of 97.8% and 99.3%. By comparison, published values of moisture content for disc-stack solids are 50–150 g/L (**4**). Extrapolating to higher cell mass fermentation lysates — e.g., 100 g/L dry solids (**20**) — the projected clarification yields would be 95% for the APD model and only 73% for a disc-stack centrifuge.

That lower liquid entrainment of the APD centrifuge is also important in isolating purified solids such as protein precipitates and inclusion bodies. For example, in a 1% suspension of precipitated product, the dry cake of an APD centrifuge affords more than 40-fold removal of impurity liquors compared with only a sevenfold removal for a disc-stack design (75 g/L). Moreover, parallel centrifuges (each fully enclosed and automated) would allow a reslurry wash step to further purify such product solids.

Shear Sensitivity: Mammalian cells are highly sensitive to fluid shear and can easily be degraded in the feed zone of a conventional centrifuge. To quantify mammalian cell breakage, we

Calculating Shear

Entrance, Feed Tube, and Acceleration on Feed Cone: Shear rates in the feed tubes are calculated from an expression derived for laminar flow in a tube (Equation 6, where $\gamma_{feed\ tube}$ is the shear rate at the tube wall, V is the average fluid velocity in the tube, and D_{tube} is the tube's internal diameter). When feed liquid strikes the centrifuge cone, it is rapidly accelerated to the bowl's speed (Equation 7, where V_{bowl} is the bowl's tangential velocity, R_5 is the bowl's radius at the feed injection site, and ω is the bowl's rotation rate). Assuming that the feed liquid retains a cylindrical shape as it strikes the bowl, shear can be approximated by Equation 8, where $\gamma_{feed/bowl}$ is the fluid strain rate as the fluid enters the bowl, $V_{bowl,feed}$ is the velocity of the bowl at the feed region, and D_{tube} is the feed tube diameter.

$$\gamma_{feed\ tube} = \frac{8V}{D_{tube}}$$

$$V_{bowl\text{-}feed} = \omega 2\pi R_5$$

$$\gamma_{feed\text{–}bowl} = \frac{V_{bowl\text{-}feed}}{D_{tube}}$$

Shear in the feed tube is about $10^2\ s^{-1}$ for all centrifuge sizes, and shear rates at the feed contact point are or the order $10^3\ s^{-1}$. Table 4 indicates that entrance shear, either in the feed tube or at the point of impact with the feed cone, does not increase in larger equipment and may actually decline.

Centrate Collection Area: Shear is likely to be greatest in the centrate region. It broke polysaccharide in the largest Powerfuge (16). High fluid wall shear is subsequent to impingement as fluid leaves stagnation point. Deshpande, et al. numerically simulated stagnation point shear (21). Represented as frictional loss, it is normalized relative to the kinetic energy of an impinging fluid. The maximum value of dimensionless wall shear (τ_w) was 0.04 (Equation 9, where r is the fluid density and V is the fluid velocity normal to the wall).

$$\frac{\tau_{wall}}{4\rho V^2} = 0.04$$

Alternatively stated, only about 4% of fluid energy reaches the stagnation point condition in a single pass. Approximating the impinging fluid velocity by the tangential bowl speed of Equation 7 (nonslip discharge), Table 4 shows that impingement shear calculated by Equation 8 is five orders of magnitude larger than for other locations, 10^7–$10^8\ s^{-1}$.

measured the concentration of host cell DNA in our centrate. Figure 3 shows no increase in soluble DNA after centrifugation. In our particle size analysis of feed and centrate streams (Figure 4), 10-µm cells from the centrifuge feed were completely removed. Figure 4 also shows that cells harvested by the novel scraper device contain the same proportion of intact 10-µm cells. We resuspended our collected paste and examined cells under a microscope for integrity, finding no loss of cell integrity even after harvest with the scraper mechanism (data not shown). The ability to discharge such undamaged cell paste is a unique advantage of the APD centrifuge.

DNA and Polysaccharides: Figure 5 is a gel electrophoresis of centrate samples taken during five-pass exposure of a plasmid DNA solution through the APD-125 centrifuge. No plasmid DNA degradation occurred due to centrifuge shear. The gel does show some increased chromosomal DNA degradation, which is to be expected because of the extreme shear sensitivity of that form. Figure 6 illustrates that there was no shear degradation of polysaccharide in a 1-g/L solution.

Discussion

Scale-Up of Throughput: Table 2 lists maximum speed and calculated maximum values of Sigma (from Equation 2) for the available APD centrifuges. All models achieve a maximum centrifugal force of 20,000 *g*. Going from the smallest development scale unit (APD-75) to the largest production scale unit (APD-375) constitutes a 25-fold increase in Sigma factor and a 120-fold increase in solids capacity. Based on the required values of Q/Σ for our experimental clarifications of *E. coli* lysate and *S. pneumoniae* flocculate, we calculated throughput values for the larger models in the APD series. As in Figure 2, our chosen values of Q/Σ were 2.8×10^{-9} m/s for *E. coli* (95% clarification), 1.4×10^{-8} m/s for *S. pneumoniae* flocculate (98% clarification), and 1.2×10^{-7} m/s for CHO cells (70% clarification of debris from centrifuge feed).

Using those projected throughput values, Table 3 estimates durations for clarifying three feed streams at different scales of operation. Sigma analysis predicts that a single centrifuge from the ADP series could be used to harvest mammalian cells within a reasonable time (<14 hrs) at development, pilot, and manufacturing scales. Likewise, a single machine would be sufficient to clarify flocculated microbial lysate at each scale. For the more difficult *E. coli* lysate clarification, an APD-75 and an APD-125 should be sufficient at development and pilot scales, respectively. However, two of the largest centrifuges are required to clarify an *E. coli* lysate at manufacturing scale within 24 hours. The narrow bowl size and automated operation of the APD are well suited for parallel or even series operation.

Sufficient solids hold-up in the APD series keeps the number of bowl discharges during batch clarification from becoming excessive and thereby constraining productive operation. The number of drops is <10 at the development and pilot scales, and only a single drop is required with the manufacturing equipment.

Analysis of Shear: Figures 3–6 show that the APD-125 centrifuge did not damage mammalian cells, plasmid DNA, or polysaccharides, all shear-sensitive compounds that have been broken in model flow systems at documented values of threshold shear. Thus, approximate hydrodynamic models of the several hot spots in a centrifuge should calculate shear rates below the published threshold values.

In the APD model, feed and collection regions provide potential conditions for shear damage: high

Table 2: Centrifuge model specifications

Model	Maximum G Force (*g*)	Maximum Speed (rpm)	Σ m^2 (m/s)	APD Relative Σ	Solids Space (L)	Bowl Radius (mm)	Bowl Radius at Cone (mm)	Feed Jet (mm)	Exit Weir Height (mm)
Powerfuge P-6	20,000	15,325	1,041	N/A	0.8	N/A	N/A	N/A	N/A
APD-75	20,000	22,000	1,748	1.0	0.9	25.0	8	3	10
APD-125	20,000	14,722	4,833	2.8	4.3	41.7	16	5	14
APD-250	20,000	11,970	19,171	11.0	34.0	83.3	32	10	28
APD-375	20,000	9,770	43,104	24.7	115.0	125.0	64	20	56

velocities and thin sheets. Feed tube fluid velocity is high simply because the entire batch is fed through a single tube. Leaving that, a thin cylinder of fluid experiences shear by being distributed onto a high-speed centrifuge bowl. Next, in the upper section of that bowl, some wall shear occurs as clarified fluid flows upward at modest velocity over a wetted cylindrical section. At the top of the bowl, that liquid film abruptly turns 90 degrees and is accelerated to the bowl's tangential speed, being ejected by centrifugal force through four slots. Finally, ejected fluid is rapidly decelerated by impingement on the wall of the centrate collection bowl.

To calculate fluid shear, we first specify liquid volumetric flow rates. Our chosen basis came from the experimentally measured value of Q/Σ: 2.8×10^{-9} m/s, corresponding to 96% clarification of *E. coli* in the APD-125 at 15,000 *g* (Figure 2). Using that value and maximum *g*-forces for the various centrifuges, we easily calculated a maximum flow rate for each one. Using those flow rates, rotational speeds, and relevant equipment dimensions, we determined shear rates in several "hot spots" for each centrifuge size. Table 4 summarizes our results, and the "Calculating Shear" box describes the methods applied.

Comparing Our Results with Published Values

Mammalian Cells: A critical wall shear rate of 10^3 s^{-1} has been measured for several types of mammalian cells (**22**). Table 4 shows that the APD feed tube shear is below that value, but shear estimated for the feed/cone bowl-contact point is within that range. The upflow design may create a thicker, flooded film on the feed cone, which allows fluid to slip as it enters the cone. But shear will be inversely related to the square of such a film's thickness.

Table 3: Cycle time and bowl drops at different scales using APD centrifuges

Material	Q/Σ (m/s)	Batch Processing Time and Number of Bowl Drops: Laboratory 50-L APD-75 (hr)	Laboratory 50-L APD-75 (Drops)	Pilot 500-L APD-125 (hr)	Pilot 500-L APD-125 (Drops)	Pilot 2000-L APD-250 (hr)	Pilot 2000-L APD-250 (Drops)	Production 15,000-L APD-375 (hr)	Production 15,000-L APD-375 (Drops)
E. coli lysate (5% wet solids)	2.8×10^{-9}	4	3	13	6	13	3	42	7
Microbe flocculate (3% wet solids)	1.4×10^{-8}	2	2	8	4	8	2	25	4
Hybridoma broth (1% wet solids)	1.2×10^{-7}	1	1	4	1	4	1	14	2

Table 4: APD model fluid shear calculations

ADP Model	Bowl Speed (rpm)	G Force at Wall (*g*)	Flow Rate (Lpm)	Shear (1/s): Feed Tube	Feed Cone	Centrate Impingement (Equation 9)	Centrate Impingement (Equation 10)	Sheet Thickness (mm)
75	22,000	20,280	0.30	1780	6140	3.8×10^8	5.0×10^8	1.3
125	17,000	20,182	0.81	1050	5700	2.9×10^8	1.6×10^8	2.8
250	12,000	20,112	3.24	526	4020	5.8×10^8	1.6×10^8	4.0
375	10,000	20,950	7.58	154	3350	16.0×10^8	3.9×10^8	2.8

Polysaccharides and Plasmid DNA: Using capillary shear, Lander et al. (**23**) found that 10^5 s^{-1} is required to break Pneumovax polysaccharides. For plasmid DNA, Levy (**15**) used a rheometer to find threshold shear values of 10^7 s^{-1} for plasmid DNA of 6–8 kbp. Calculated shear rates in the feed region do not exceed those values, but those in the impingement section are one or two orders of magnitude larger than the plasmid DNA and polysaccharide breakage threshold values, respectively.

Despite that excessive calculated shear rate in the impingement section, both DNA (multipass) and polysaccharide molecules remained intact. Several explanations are possible. First, residence time in the impingement area is very short. In a similar period, however, the Powerfuge P24 broke polysaccharides (**16**). So it is more likely that our calculation of shear is very conservative.

Impingement also can be estimated by assuming that fluid leaves the bowl as a sheet spread out over the four holes or the entire bowl circumference in the case of "low-shear" discharge.

Equation 10

$$\delta = \frac{Q}{V_{fluid} \times 4 J_w}$$

The thickness of such a sheet is given by Equation 10, where V_{fluid} equals $2\pi R\omega$ and J_w is the width of the four discharge slots. In fact, depending on how fluid splashes at impact, impingement shear can vary by as much as five orders of magnitude.

As Table 4 shows, a large tangential bowl velocity causes the fluid to become very thin (~10 µm). Shear is then estimated by forming the ratio of Equation 8 but substituting the tangential bowl speed and sheet thickness from Table 4. The result is about the same as from the energy-based method of Deshpande (**21**), ~10^8 s^{-1}.

Both impact energy and fluid sheet approximations yield shear rates that far exceed the threshold breakage value of polysaccharide and even plasmid DNA. So an alternative explanation is needed. After studying the Powerfuge, Dieter et al. (**16**) suggested that centrate liquid is so thin that it breaks up into droplets. Those would be

readily decelerated by drag reduction in the vapor space before striking a collection wall, thereby lowering shear on impact. Given the thin sheet calculated in Table 4, it seems likely that this mechanism was also present in our experiments.

An Attractive Alternative

We found the APD model to be a flexible centrifuge offering the separation advantage of narrow-bowl geometry (like the historical Sharples design) with fully enclosed operation and automated CIP/SIP cleaning capability. The machine successfully clarified a range of different feed streams. Based on Sigma analysis, it should be capable of clarifying bioprocess streams from development to manufacturing scales. So we see this centrifuge as an excellent choice for multiproduct facilities making clinical supplies or marketed drugs.

APD centrifuges have solids-related advantages over disc-stack designs. A very dry centrifuge cake is produced, enabling the highest possible product yields for clarification of desirable, high–cell-density fermentations. The relatively dry discharged paste also assures maximum purification for isolation of solid-phase products such as protein precipitates and inclusion bodies. And this centrifuge has recovered intact mammalian cells as a paste with its gentle piston discharge, which suggests a unique potential for harvest of very sensitive cells. Finally, the simple and thorough discharge should permit superior solids recovery, important for single-drop processing of low-volume/high-value biological solid products.

Because of its narrower bowl construction and piston discharge, this design offers several other advantages over competing tubular bowl and disc-stack machines:

- a higher upper limit of centrifugal force, eliminating the requirement of, for example, titanium construction materials
- the largest bowl (115 L maximum) is two times larger than the largest Powerfuge
- the unbaffled bowl offers excellent rapid cake clearance and evident advantages in cleaning, particularly compared with the complex internal construction of a disc-stack centrifuge
- upflow operation promotes a more stable liquid pool and a more flooded, lowered shear condition for the feed cone.

Calculations of shear in putative hot spots suggest that only the product collection area, where high-speed discharged centrate impinges on the casing wall, can produce shear sufficient to break polysaccharides or plasmid DNA. But recycled plasmid DNA did not break in the APD-125, and we have proposed a plausible hydrodynamic model to explain this.

Scale-up should be straightforward because the internal design of APD centrifuges is identical to the industry-standard Sharples model. As with that historical predecessor, we can envision parallel arrangements making possible even greater throughput, solids washing steps, and enhanced clarification in series.

Acknowledgments

The authors are grateful to Amy Bowman and Matt Watson of Merck & Co. and to Gary Brown of Celeros.

References

1 Van Reiss R, et al. High Performance Tangential Filtration. *Biotechnol. Bioeng.* 56(1) 1997: 71– 82.

2 Meacle F, et al. Optimization of the Membrane Purification of a Polysaccharide-Protein Conjugate Vaccine Using Backpulsing. *J. Membrane Sci.* 161, 1997: 171–184.

3 Van Reiss R. *Tangential Flow Filtration Process and Apparatus.* US Patent 5,490,937 (Genentech, Inc.) 13 February 1996.

4 Axelsson H. Cell Separation, Centrifugation. *The Encyclopedia of Bioprocess Technology: Fermentation, Biocatalysis, and Bioseparation.* Flickinger MC, Drew SW, Eds. John Wiley & Sons, Inc.: New York, NY, 1999.

5 Winters C. Development, Characterization, Validation, and Implementation of Genentech's CHO Harvest Operations. *Abstracts of Papers: 227th ACS National Meeting,* Anaheim, CA, 28 March – 1 April 2004. American Chemical Society: www.chemistry.org.

6 Castillo LR, Medronho RA. Cell Retention Devices for Suspended Cell Perfusion Cultures. *Adv. Biochem. Eng. Biotechnol.* 74, 2002: 131.

7 Kempken R, Preibmann A, Berthold W. Clarification of Animal Cell Cultures on a Large Scale By Continuous Centrifugation. *J. Indust. Microbiol.* 14, 1995: 52.

8 Tebbe H, et al. Gentle Separation of Hybridoma Cells By Continuous Disc Stack Centrifugation (submitted).

9 Hamamoto K, Ishimaru K, Tokashiki M. Perfusion Culture of Hybridoma Cells Using a Centrifuge to Separate Cells from Culture Mixture. *Cytotechnol.* 3, 1990: 329.

10 Shpritzer R, et al. Evaluation of a Continuous Disc Stack Centrifuge for the Clarification of Mammalian Cell Cultures. Presented at *225th ACS National Meeting,* New Orleans, 24 March 2003 (American Chemical Society, Washington, DC; www.chemistry.org).

11 Pham C, et al. Solid–Liquid Separation of Mammalian Cell Culture Suspensions Using a Continuous Disk Stack Centrifuge. Presented at *Recovery and Purification,* 18 November 2002 (IBC Life Sciences, Westborough, MA; www.lifesciencesinfo.com).

12 Wong HH, O'Neill BK, Middelburg APJ. Centrifugal Processing of Cell Debris and Inclusion Bodies from Recombinant *Escherichia coli*. *Bioseparation* 6(6) 1996: 361–372.

13 Tinnes R, Hoare M. The Biocontainment of a High Speed Disc Bowl Centrifuge. *Bioprocess Eng.* 8, 1992: 165.

14 Leneweit G, et al. Shear Degradation and Deformation of Polysaccharides in Thin Liquid Film Flow on a Rotating Disk. *Polymer Degrad. Stability* 70(2) 2000: 283–297.

15 Levy MS. Effect of Shear on Plasmid DNA in Solution. *Bioprocess Eng.* 20, 1999: 7–13.

16 Pujar N, Dieter L. Merck internal document (untitled as of 6 October 2005, to be published).

17 Bednar B, Hennessey JP. Molecular Size Analysis of Capsular Polysaccharide Preparations from *Streptococcus pneumoniae*. *Carbohydr. Res.* 243, 1993: 115–130.

18 Maybury JP, Hoare M, Dunnill P. The Use of Laboratory Centrifugation Studies to Predict the Performance of Industrial Machines: Studies of Shear Insensitive and Shear Sensitive Materials. *Biotechnol. Bioeng.* 67, 2000: 265.

19 Ambler CM. The Evaluation of Centrifuge Performance. *Chem. Eng. Progr.* 150, March 1952.

20 Squires CH, et al. Heterologous Protein Production in *P. fluorescens*. *BioProcess International* 2(11) 2004: 54–59.

21 Deshpande MD, Vaishnav RN. Submerged Laminar Jet Impingement on a Plane. *J. Fluid. Mech.* 114, 1982: 213–236.

22 Maiorella B, et al. Crossflow Microfiltration of Animal Cells. *Biotechnol. Bioeng.* 37, 1990: 121–126.

23 Lander R, et al. Gaulin Homogenization: A Mechanistic Study. *Biotechnol. Progr.* 16, 2000: 80–85.

***Russ Lander** is a senior investigator, **Chris Daniels** is a research biochemical engineer, and corresponding author **Francis Meacle** is a senior research biochemical engineer in biologics development and engineering at Merck & Co., WP17-301, Westpoint, PA 19486; 1-215-652-5848, fax 1-215-993-4911, francis_meacle@merck.com.*